Published in final edited form as:
Arch Biochem Biophys. 2013 September 15; 537(2): . doi:10.1016/j.abb.2013.07.013.

Structural basis for the *in situ* Ca^{2+} sensitization of cardiac troponin C by positive feedback from force-generating myosin cross-bridges

Daniel C. Rieck[†], **King-Lun Li**[†], **Yexin Ouyang**[‡], **R. John Solaro**[§], and **Wen-Ji Dong**[†,‡,*]

[†]Gene and Linda Voiland School of Chemical Engineering and Bioengineering, Washington State University, Pullman, WA 99164, USA

[‡]Department of Integrated Physiology and Neuroscience, Washington State University, Pullman, WA 99164, USA

[§]Department of Physiology and Biophysics, Center for Cardiovascular Research, University of Illinois at Chicago, Chicago, IL 60612, USA

Abstract

The *in situ* structural coupling between the cardiac troponin (cTn) Ca^{2+}-sensitive regulatory switch (CRS) and strong myosin cross-bridges was investigated using Förster resonance energy transfer (FRET). The double cysteine mutant cTnC(T13C/N51C) was fluorescently labeled with the FRET pair 5-(iodoacetamidoethyl)aminonaphthelene-1-sulfonic acid (IAEDENS) and N-(4-dimethylamino-3,5-dinitrophenyl)maleimide (DDPM) and then incorporated into detergent skinned left ventricular papillary fiber bundles. Ca^{2+} titrations of cTnC(T13C/N51C)$_{AEDENS/DDPM}$-reconstituted fibers showed that the Ca^{2+}-dependence of the opening of the N-domain of cTnC (N-cTnC) statistically matched the force–Ca^{2+} relationship. N-cTnC opening still occurred steeply during Ca^{2+} titrations in the presence of 1 mM vanadate, but the maximal extent of ensemble-averaged N-cTnC opening and the Ca^{2+}-sensitivity of the CRS were significantly reduced. At nanomolar, resting Ca^{2+} levels, treatment with ADP•Mg in the absence of ATP caused a partial opening of N-cTnC. During subsequent Ca^{2+} titrations in the presence of ADP•Mg and absence of ATP, further N-cTnC opening was stimulated as the CRS responded to Ca^{2+} with increased Ca^{2+}-sensitivity and reduced steepness. These findings supported our hypothesis here that strong cross-bridge interactions with the cardiac thin filament exert a Ca^{2+}-sensitizing effect on the CRS by stabilizing the interaction between the exposed hydrophobic patch of N-cTnC and the switch region of cTnI.

Keywords

cardiac troponin; thin filament regulation; myosin cross-bridges; FRET; cardiac muscle

[*]Correspondence: wdong@vetmed.wsu.edu.

Introduction

Phenomenological evidence has long pointed toward the ability of force-generating, strong myosin cross-bridges (XBs) to exerting a positive, activating feedback on myocardial contractile regulation [1-6]. This positive feedback mechanism is uniquely important to the physiological function of cardiac muscle [6,7], and understanding its molecular basis is thus a goal of considerable therapeutic potential [8]. Myocardial contractile regulation is traced to cardiac troponin (cTn), which is the protein complex that responds to sarcomeric Ca^{2+} signals in regulating the ability of XBs to interact with the cardiac thin filament and generate force. The cTn complex is a ternary heteromer [9,10] whose subunits include: cTnC, a calmodulin-like Ca^{2+}-sensing protein; cTnI, an adaptor protein whose interactions with other thin filament proteins are Ca^{2+} dependent, and which works in concert with tropomyosin to inhibit the XB cycle; and cTnT, another adaptor protein that integrates the cTn complex into the ultrastructure of the thin filament. Therefore, cTn may be thought of as a binary, “activate/deactivate” Ca^{2+}-sensitive regulatory switch (CRS) [11,12] whose function essentially involves a conformational signaling process driven principally by a Ca^{2+} chelation reaction. The terminal, critical structural outcome of this conformational signaling is a change in the steric accessibility of myosin binding sites on actin to XBs [13,14].

The conformational changes by which the activating CRS signal leads to interactions between strong cycling XBs and the thin filament have been well characterized by *in vitro* biophysical studies. In the absence of Ca^{2+}, the C-terminal cTnI inhibitory region (cTnI-IR; residues 130–150) and mobile domain (cTnI-MD; residues 168–210) are both bound to actin [15]. This confines the azimuthal position of tropomyosin on actin over myosin binding sites [16] in what is known as the blocked state of the three-state model of thin filament regulation [17,18]. Activation is initiated through a drag-and-release mechanism [8,11,19], wherein N-cTnC binds to the cTnI switch region (cTnI-SR; residues 151–167) and consequently “drags” on cTnI to “release” the actomyosin-ATPase inhibitory interactions between cTnI and actin. The N-cTnC-cTnI-SR interaction that is central to this mechanism is triggered by the binding of Ca^{2+} to N-cTnC. This stimulates N-cTnC to sample an open conformation [20-22] wherein its buried hydrophobic core becomes a surface exposed hydrophobic patch ready for interaction with cTnI-SR. Open N-cTnC conformers are then conformationally selected by the binding of cTnI-SR to the exposed hydrophobic patch [22]. The N-cTnC–cTnI-SR interaction thus simultaneously stabilizes the Ca^{2+}-bound, open N-cTnC conformation [5,22] and destabilizes the blocked-state actin–cTnI-IR and actin–cTnI-MD interactions [19,23]. Repositioning of cTnI on the thin filament enables tropomyosin to move to a “closed-state” position [17,18] wherein the myosin binding sites of actin are partially uncovered. It has been suggested that Ca^{2+} binding alone may not completely stabilize these structural changes, such that the thin filament could be left in a conformational equilibrium between its blocked and closed states [11,12]. In any case, the structural changes stimulated by Ca^{2+} binding enable myosin heads to thereafter bind to actin and interact as strong XBs that induce additional azimuthal movement of tropomyosin to an “open-state” position [17,18]. Since myosin binding sites are completely uncovered and Ca^{2+} binding is significantly enhanced in the open-state, it is this myosin-induced movement of tropomyosin from the closed- to open-state position that is implicated as the source of positive feedback from strong XBs [5,8].

Numerous *in vitro* structural studies conducted in reconstituted thin filaments have also shown that strong XBs exert structural effects on cTn that are consistent with the positive feedback mechanism. It was shown through Förster resonance energy transfer (FRET) that, when averaging over the observed molecular ensemble, the presence of S1•ADP during Ca^{2+} titrations shifts cTnI further away from actin [23] and closer toward N-cTnC [11].

Based on electron microscopy [13] and fluorescence polarization [19] studies, this is caused by S1-mediated disruption of the closed-state interactions between actin and cTnI-MD that are associated with the fly casting mechanism [24]. The consequently increased capacity for localization between N-cTnC and cTnI-SR thus stabilizes (*i.e.* makes more stable) the Ca^{2+}-sensitizing N-cTnC–cTnI-SR interaction [11,19,25,26]. Such S1-induced stabilization of the N-cTnC–cTnI-SR interaction is also evidenced by an increased Ca^{2+}-sensitivity of CRS signaling [27,28], slowed kinetics of the deactivating CRS signal [19,25,27], and reduced exposure of cTnI-SR to solvent [19]. *In vitro* biophysical studies thus implicate strong XB induced stabilization of the N-cTnC–cTnI-SR interaction as the source of the positive feedback mechanism [7,19] and the hysteresis [29,30] observed in the N-cTnC–Ca^{2+} chelation reaction. However, it is not yet clear how structural interpretations based on *in vitro* data would hold in the myofilament lattice (which we refer to as *in situ*)[31].

Though some *in situ* biophysical studies have indicated that the positive feedback mechanism affects cTnC structure in the molecular environment of the sarcomere, the structural information provided has been less mechanistically clear due to the nature of the techniques used. Smith *et al.* tested for changes induced by orthovanadate (Vi) in the *in situ* dichroism of fluorescently labeled cTnC(C35S) [32]. They determined that ~87% of the structural change signal associated with maximal thin filament activation was due to Ca^{2+} binding, with the remaining ~13% attributable to the positive feedback mechanism; due to the nature of dichroism, it was difficult to connect these changes in signal to specific changes in thin filament activation states. In a different study by another laboratory, *in situ* fluorescence polarization measurements were conducted by Sun *et al.* to determine the effects of strong XB interactions on N-cTnC structure [31]. They labeled the C and E helices each with bifunctional rhodamine, and found through the use of blebbistatin and rigor that strong XBs stimulate additional changes in C and E helix orientation beyond what is induced by Ca^{2+} binding alone. Interestingly, their data challenged the long hypothesized role of strong XBs in the cooperative activation of the cardiac thin filament [4,33,34]. However, it was unclear how the orientational changes they observed relate to the *in vitro* conformational behavior of N-cTnC, and they recommended future studies accordingly. Therefore, it is still unknown how the geometric and mechanical constraints of the myofilament lattice may affect the N-cTnC–cTnI-SR interaction, or whether *in situ* evidence will affirm strong XB induced stabilization of the N-cTnC–cTnI-SR interaction as the structural basis for the positive feedback mechanism in cardiac muscle.

In this biophysical study, the *in situ* structural coupling between the cTn CRS and strong XBs was examined using FRET spectroscopy. We hypothesized that strong XB interactions with the cardiac thin filament exert a Ca^{2+}-sensitizing effect on the CRS by stabilizing the interaction between the exposed hydrophobic patch of N-cTnC and cTnI-SR. This hypothesis was formed based on reasoning that strong XB attachment could stabilize the N-cTnC–cTnI-SR interaction in two possible ways. Based on observations of the conformational behavior of the CRS, some biophysical evidence has suggested that the Ca^{2+} saturated thin filament could be in a conformational equilibrium between its blocked and closed states in the absence of strong XB attachment [11,12,22,35]. Therefore, one form of stabilization could be that strong XBs indirectly stabilize the open conformation of N-cTnC by moving tropomyosin to the open-state position. Such tropomyosin movement would exert a disrupting effect on the cTnI–actin interactions that counterbalance the N-cTnC–cTnI-SR interaction, thereby increasing the availability of cTnI-SR to interact with the hydrophobic patch of N-cTnC. A second form of stabilization is also possible, wherein strong XBs would induce a tightening of the N-cTnC–cTnI-SR interaction itself by disrupting the counterbalancing constraints on cTnI-SR [20,32]. Strong XBs could thus indirectly increase the “openness” of N-cTnC molecules bound to cTnI-SR. Increased ensemble-averaged hydrophobic patch exposure and enhanced CRS Ca^{2+}-sensitivity [11,12]

should result from either possible form of the hypothesized strong XB induced stabilization of the N-cTnC–cTnI-SR interaction.

In order to test our hypothesis, a double cysteine mutant cTnC(T13C/N51C) was labeled with the FRET pair 5-((((iodoacetyl)amino)ethyl)amino)naphthalene-1-sulfonic acid (IAEDENS) and (4-dimethyl-amino-3,5-dinitrophenyl)-maleimide (DDPM) [28] (Fig. 1a) and incorporated into dissected, permeabilized left ventricular papillary myocardium from *Rattus norvegicus*. As used in study, this FRET labeled N-cTnC mutant simultaneously provides information on two aspects of N-cTnC structure: 1) the fraction of molecules in the N-cTnC ensemble that are in the open conformation, and 2) the extent of separation between Cys-13 and Cys-51 that is associated with the open conformation of N-cTnC [11,12]._In our experiments, the effect of Ca^{2+}-binding on ensemble-averaged N-cTnC opening was isolated from the effect of strong XB interactions with the thin filament by conducting Ca^{2+} titrations in the absence or presence of either Vi or ADP•Mg. Ca^{2+}-titration experiments were controlled with regard to potential effects from cTnC variants, labeling, and reconstitution into myocardial fibers. Our *in situ* FRET results supported our hypothesis that the positive feedback mechanism is m ediated by the stabilizing effect of strong XBs on the N-cTnC–cTnI-SR interaction. The ensemble-averaged extent of N-cTnC opening was both highly sensitive to strong XB interactions and also positively correlated with the Ca^{2+}-sensitivity of CRS signaling. Interestingly, our results also indicated that strong XB interactions were not needed for the cardiac thin filament to activate cooperatively, and the positive feedback mechanism was confined to the A-band in the myofilament lattice.

Materials and Methods

Expression, purification, and fluorescence labeling of recombinant rat cTnC

As previously described, the double cysteine cTnC(T13C/N51C) mutant (with endogenous Cys-35 and Cys-84 both mutated to Ser) used in this study was generated from a wild-type rat cTnC clone using site-directed mutagenesis and then fluorescently labeled [28]. The two cysteine residues of cTnC(T13C/N51C) were modified such that AEDENS (FRET donor; λ_{ex} = 340 nm, λ_{em} = 480 nm) was attached to one residue and DDPM (non-fluorescent FRET acceptor) was attached to the other cysteine, producing cTnC(T13C/N51C)$_{AEDENS\text{-}DDPM}$ ($cTnC_{FRET}$). In this donor-quenching FRET scheme (Fig. 1a), the experimentalist can observe FRET by monitoring AEDENS fluorescence intensity alone. Increases in fluorescence intensity thus indicate decreases in FRET and, therefore, increased separation between Cys-13 and Cys-51 of N-cTnC.

Briefly, FRET labeling was conducted as follows. Sulfhydryl-reduced cTnC(T13C/N51C) was first reacted with a twofold molar excess of IAEDENS. The singly labeled fraction of cTnC(T13C/N51C) in the product was isolated from unlabeled and doubly labeled fractions using a DEAE column. The labeling ratio of the purified, singly labeled fraction was verified to be >95% using UV-Vis spectroscopy and $\varepsilon_{325\ nm}$ = 6000 $cm^{-1}\cdot M^{-1}$. An aliquot of cTnC(T13C/N51C)$_{AEDENS}$ was kept as a donor-only sample for reference, and the remainder was incubated with a large molar excess of DDPM to ensure that labeling of the free remaining cysteine residue occurred completely. The identity of the $cTnC_{FRET}$ product was verified using electrospray mass spectrometric analyses. The ability of $cTnC_{FRET}$ to sense N-domain opening *via* FRET was verified *in vitro* by fluorescence lifetime measurements in Ca^{2+} free or saturated conditions in the presence of cTnI(wt) from *Rattus norvegicus* (data not shown).

Preparation of detergent-skinned left ventricular myocardial fibers

All procedures for animal handling and use conformed to the guidelines of the Washington State University Institutional Care and Use Committee, and all procedures were previously approved by the Committee. Animals used in these studies were adult, untreated, and normal Sprague-Dawley rats. Rat myocardium was isolated following slightly modified, previously described procedures (25). Hearts were rapidly excised and placed into ice-cold highly relaxing (HR) solution containing butanedione monoxime (HR+BDM), with composition (in mM): 50 BES (pH = 7.00), 2 EGTA, 5 NTA, 0.005 $CaCl_2$, 5 $MgCl_2$, 5.63 Na_2ATP, 90.6 K^+-Propionate (ionic strength = 180 mM), 5 NaN_3, 1 DTT, 0.2 PMSF, and 10 2,3-butanedione monoxime (BDM). This formulation of HR solution was based on the recommendations of the Potter lab [36]. Protease inhibitors (PI) were also added to the solution as follows (in mM): 25 bestatin, 10 E-64, 10 leupeptin, 1 pepstatin [37]. Papillary muscle bundles were removed from the left ventricle of excised hearts and dissected in HR+BDM+PI under a microscope into myocardial fibers that were ∼150 μm in cross sectional diameter and ∼2 mm in length. Myocardial fibers were skinned in ice-cold HR+BDM + 1% Triton-X 100 + protease inhibitors. Fibers were immediately used for experiments within 3 days, and were kept stored at 4 °C in HR+BDM+PI when not being handled.

Incorporation of fluorescently labeled cTnC constructs into skinned myocardial fibers

Detergent skinned fibers were first incubated for 120 minutes at 23 °C under gentle shaking in a cTnC extraction buffer containing (in mM): 5 1,2-cyclohexylenedinitrilotetraacetic acid, 40 Tris-HCl (pH 8.4), 0.6 NaN_3, and 0.1 DTT [38]. Fibers were then washed three times, wherein each wash consisted of incubating the fibers in fresh HR+BDM+PI at 23 °C under gentle shaking for 5 minutes. Some fibers were retained as a cTnC-depleted control to verify the extent of cTnC extraction. Remaining cTnC-extracted fibers were incubated overnight at 4 °C in HR+BDM+PI containing 1.2 $mg{\cdot}mL^{-1}$ of the desired exogenous cTnC construct [38] and 0.76 $mg{\cdot}mL^{-1}$ of wild type myosin regulatory light chain [39]. Before handling cTnC-reconstituted fibers further, fibers were washed three times in fresh HR+BDM as above, then stored at 4 °C in HR+BDM+PI. Fibers reconstituted with $cTnC_{FRET}$ were used for monitoring changes in the average, steady-state extent of *in situ* opening of N-cTnC and concomitant exposure of its hydrophobic patch. Fibers reconstituted with $cTnC(T13C/N51C)_{AEDENS}$ were prepared as a donor-only sample to verify that changes in fluorescence intensity observed from $cTnC_{FRET}$-reconstituted fibers were due to changes in FRET. Fibers reconstituted with cTnC(wt) were used to control for the effects of reconstitution and mutation and fluorophore labeling of cTnC.

The extents of cTnC extraction and reconstitution achieved using this protocol were determined by SDS-PAGE, Western blotting, and densitometry [37] (Fig. 1). Briefly, a group of fibers was incubated in a 10 μL/fiber volume of protein extraction buffer (40 mM MOPS pH 6.8, 10% w/v glycerol, 1 mM DTT, 2.5% SDS) for 1 hour at 4 °C. The resulting protein extraction sample was then sonicated at 4 °C for 20 min and clarified by centrifugation at 13,000 RPM for 10 min at 4 °C. An equal volume of 2× Laemmli buffer (60 mM Tris-HCl pH 6.8, 2% SDS, 10% w/v glycerol, 0.1% bromophenyl blue) was added to the protein extraction sample, which was then heated at 95 °C for 5 min. Protein extraction samples were then loaded into a 15% acrylamide gel, after which extracted proteins were separated by SDS-PAGE. The resulting gel was stained with SYRPO Tangerine (Life Technologies) and imaged using a Universal Hood II gel imager (Bio-Rad) for visualization of total protein loading. Following visualization, proteins in the gel were transferred to a nitrocellulose membrane which was then Western blotted with antibody against cTnC (#10-T78A, Fitzgerald Industries International). Horseradish peroxidase conjugated secondary antibody against mouse IgG (GE Healthcare), Pierce Enhanced

Chemiluminescent substrate (Thermo Scientific) and the Universal Hood II were then used to image cTnC bands.

Measurement of *in situ* N-cTnC opening using FRET, Ca^{2+}-titrations and chemical modulators of the cross-bridge cycle

To conduct synchronized tension and *in situ* fluorescence spectroscopy measurements, calcium titrations were performed using a Güth Muscle Research System (MRS) OPT (Scientific Instruments, Heidelberg, Germany) and methods similar to what is described by the Kerrick lab [40]. The MRS OPT is equipped with a PH1A microscope photometer located directly above a quartz perfusion cuvette. An HBO100 mercury high pressure burner is situated behind the cuvette, from the experimentalist's perspective, and provides excitation light. Before experiments for the day were started, the HBO100 was allowed to warm up for 30 minutes. When testing a fiber, it was first suspended in the cuvette between a KG7B force transducer and a micrometer using “hockey stick” tweezer mounts. The microscope was used to carefully align the fiber in the imaging window of the photometer. Dorsally and laterally oriented pictures were taken of the fiber using a distance calibrated MoticCam 2000 microscope camera (Motic Group Co., Ltd., Xiamen, China). These pictures were used to calculate the fiber's cross sectional area under the assumption that fibers are elliptically shaped. Sarcomere length was set to 2.3 μm using laser diffraction, and the fiber was then ready for testing.

Our protocol for the synchronous measurement of force and fluorescence intensity was similar to how the optical Güth system is classically used to simultaneously measure skinned fiber force and ATPase activity from NADH fluorescence [41]. While steady-state fiber force was being measured by the MRS force transducer during a test, fluorescence was being synchronously measured with the PH1A microscope photometer. The MRS was covered with black cloth and its room was kept dark during measurements. Mounted fibers were monitored for bulk emission >400 nm from FRET donor AEDENS using a cutoff optical filter and the PH1A photometer. AEDENS was excited at 343 nm using a shortpass filter and the HBO100. Preliminary tests were performed on skinned fibers reconstituted with $cTnC(T13C/N51C)_{AEDENS}$ in order to adjust the position of the condenser of the HBO100 lamp housing to produce general fiber emissions of optimum intensity. Such fibers were used for this purpose because they produced the most intense signals during our study due to the absence of the DDPM acceptor fluorophore, which quenches AEDENS fluorescence *via* FRET. After adjustment of the condenser, its position was maintained throughout the remainder of the study to ensure a consistent intensity of excitation light between experiments.

Fiber testing was generally conducted as follows. An initial contraction of the fiber was performed using a maximally activating solution (pCa = 4.3), during which the maximal stress and fluorescence intensity were recorded. The fiber was then relaxed using HR. Proper sarcomere length was verified and a Ca^{2+} titration was then performed using solution peristaltically pumped from an MRS Ca^{2+} concentration gradient maker [40]. As described by Allen *et al.*, the gradient maker (depicted in Fig. 2A) consists of a lower, flow-through solution chamber that is equipped with a magnetic stirrer and connected to an upper solution chamber by a capillary channel. Each Ca^{2+}-titration experiment was started with HR solution loaded into the lower mixing chamber of the gradient maker and a high-Ca^{2+}, gradient generating solution (pCa = 3) loaded into its upper chamber. A peristaltic pump controlled by compter was used to pump a fixed volume of solution (~50 μL) out of the lower mixing chamber and toward the downstream perfusion cuvette every 15 seconds. This pumping step also simultaneously draws the same volume of gradient generating solution out of the upper chamber and into the lower flow-through chamber, which increases the Ca^{2+} level of the solution in the lower chamber. Plugs of solution were thus sequentially

delivered to the mounted fiber contained in the optical cuvette wherein each plug had a higher Ca^{2+} level than the last. The Ca^{2+} gradient that results from this scheme was calibrated using fluorescent Ca^{2+} indicator calcium-green-2 (cell impermeable, Molecular Probes) excited at 480 nm with emission monitored above 515 nm [40] (Fig. 2A). After a five sec delay following each pumping step, the steady-state fiber stress and fluorescence intensity resulting from the new Ca^{2+} level in the cuvette was simultaneously measured over a 10 sec interval.

To test for the effect of strong XB interactions on Ca^{2+}-dependent, *in situ* N-cTnC opening, chemical modulators of XB cycling were used. Thin filament activation was tested under conditions of "normal" XB cycling in the absence of modulators, a fully inhibited XB cycle, and maximal attachment of non-cycling strong XBs using 5.63 mM ATP, 1 mM sodium Vi, and 5 mM ADP•Mg + 0 mM ATP respectively. Tests using XB cycle modulators started with an initial contraction in the absence of the modulator followed by relaxation. HR containing the modulator was then flushed into the perfusion cuvette. A Ca^{2+} titration was performed wherein the Ca^{2+} gradient was generated from HR and gradient generating solution containing the modulator. In the case of Vi and under the experimental conditions used, neither appreciable Vi-mediated extraction of cTnC [42] nor any significant effect from Vi-mediated photocleavage of myosin [43-45] took place in the Vi-treated sample group based on Vi-free Ca^{2+}-titrations conducted immediately following tests in the presence of Vi. No significant differences in passive force, contractility or maximal force were observed during these follow-up titrations relative to Ca^{2+}-titrations performed on cTnC(wt)-reconstituted fibers ($p > 0.05$, data not shown). The maximal fluorescence intensity observed during follow-up titrations and the initial contraction was also not significantly different. The apparent lack of significant Vi-mediated photocleavage of myosin was attributed to the continual presence of actin and ATP, which inhibit photocleavage [46], during Vi-treated Ca^{2+}-titrations.

Statistical analysis

Data describing the Ca^{2+} -dependence of the myocardial fiber stress or AEDENS fluorescence intensity observed in our different sample groups were fit with a single Hill equation using nonlinear regression:

$$\theta\left(\left[\mathrm{Ca}^{2+}\right]\right) = (\theta_{\max} - \theta_{\min}) \frac{\left[\mathrm{Ca}^{2+}\right]^{\mathrm{n_H}}}{\left(10^{-\mathrm{pCa_{50}}}\right)^{\mathrm{n_H}} + \left[\mathrm{Ca}^{2+}\right]^{\mathrm{n_H}}} + \theta_{\min}, \quad (1)$$

where θ_{min} represents normalized passive stress or minimal fluorescence intensity, θ_{max} the normalized maximal stress or maximal fluorescence intensity, pCa_{50} the negative log of the $[Ca^{2+}]$ producing half maximal change in stress or fluorescence, and n_H the Hill coefficient. All fiber data that was included in fitting exhibited less than 20% run down, which was determined by comparing the maximal stress observed during the initial contraction with that observed at the end of the last Ca^{2+} titration performed on the fiber. Best fit parameter values are expressed as means ± SE, and the statistical significance of parameter comparisons was determined based on a two-tailed Student's *t* test.

As described further in our results section, fluorescence intensity data from ADP•Mg treated, $cTnC_{FRET}$ reconstituted fibers was indicative of two distinct conformational populations of cTn molecules. Two-population conformational behavior was also noted by Sun *et al.* in their fluorescence polarization data from Ca^{2+} titrations conducted in rigor [31]. Sun *et al.* demonstrated that a model consisting of a weighted sum of two Hill equations proved more effective than a single Hill equation at describing N-cTnC conformational

changes under rigor. As described further by Sun *et al.*[31], a weighted sum of two Hill equations accounts for the fact that the thick filament does not extend into the I-band to overlap with the thin filament. This necessitates the absence of the positive feedback mechanism as a factor in the conformational behavior of cTn molecules located in the I-band; therefore, two conformational populations of N-cTnC molecules should exist under conditions of either rigor or non-cycling strong XBs. Mathematically, the model takes the form:

$$\theta\left(\left[\mathrm{Ca}^{2+}\right]\right)=(\theta_{\max}-\theta_{\min})\left(\frac{\alpha\left[\mathrm{Ca}^{2+}\right]^{\mathrm{n_{H,\,A}}}}{\left(10^{-\mathrm{pCa_{50,\,A}}}\right)^{\mathrm{n_{H,\,A}}}+\left[\mathrm{Ca}^{2+}\right]^{\mathrm{n_{H,\,A}}}}+\frac{(1-\alpha)\left[\mathrm{Ca}^{2+}\right]^{\mathrm{n_{H,\,I}}}}{\left(10^{-\mathrm{pCa_{50,\,I}}}\right)^{\mathrm{n_{H,\,I}}}+\left[\mathrm{Ca}^{2+}\right]^{\mathrm{n_{H,I}}}}\right)+\theta_{\min},\quad(2)$$

where θ_{min}, θ_{max}, n_H, and pCa_{50} are the same as described in Eq. 1; contractility parameters denoted with an “A” or “I” refer to cTnC molecules located in the A-band or I-band, respectively; and α refers to the fraction of cTnC molecules that are located in the A-band.

When fitting Eqn. 2 to our ADP•Mg treated, $cTnC_{FRET}$ reconstituted fiber data, Akaike information criteria (AIC) [47] were used to compare the effectiveness of Eqn. 2 to Eqn. 1 as models. The AIC is based on Kullback-Leibler information and provides an asymptotically unbiased and relative estimator of the information lost when a model is used to describe reality [48]. For a particular candidate model, an AIC value may be calculated from the equation:

$$\mathrm{AIC}=2\mathrm{k}+\mathrm{n}\left[\ln\left(\frac{2\pi\cdot\mathrm{SSE}}{\mathrm{n}}\right)+1\right],\quad(3)$$

where SSE is the sum of squared errors of prediction, k is the number of model parameters, and n is the number of observations. Taking AIC_{min} to represent the minimum AIC value obtained from among all models being considered, the relative probability [48,49], or p_i, that the i^{th} candidate model will be as likely to minimize information loss was determined according to the equation:

$$\mathrm{p_i}=\mathrm{e}^{\frac{\mathrm{AIC_{min}}-\mathrm{AIC_i}}{2}}\quad(4)$$

Results

$cTnC(T13C/N51C)_{AEDENS/DDPM}$ was efficiently incorporated into skinned fibers

Since our experiments were designed to rely upon an extraction/reconstitution strategy to incorporate exogenous, fluorescently labeled cTnC constructs into myocardial fibers, it was important to determine the effectiveness of our reconstitution protocol. SDS-PAGE and Western blotting were used accordingly to separate and quantify sarcomeric proteins extracted from detergent skinned (n = 6), CDTA treated (n = 6), and $cTnC_{FRET}$ reconstituted (n = 6) fibers (Fig. 1b). These samples were prepared from the left ventricular papillary muscle from a single rat heart. Densitometric comparison of the cTnC bands in the detergent skinned and CDTA treated fiber lanes determined that 84.1% of the endogenous cTnC molecules were extracted by CDTA. Comparison of the untreated and $cTnC_{FRET}$ reconstituted fiber lanes found that 94.1% of the removed cTnC molecules were replaced with $cTnC_{FRET}$, for a final reconstitution efficiency of 94.2%. This implied that $cTnC_{FRET}$ was ~5 fold more abundant in the reconstituted fibers than residual endogenous cTnC. Our

reconstitution protocol was thus highly effective, resulting in a high degree of exogenous cTnC incorporation at the cost of a loss of cTnC molecules from only ~6% of the regulatory units present in the fiber. It was also noted that mounted myocardial fibers reconstituted with $cTnC_{FRET}$ and donor-only $cTnC(T13C/N51C)_{AEDENS}$ were visibly, intensely, and uniformly fluorescent when illuminated by UV light (Fig. 1c).

Reconstitution with $cTnC(T13C/N51C)_{AEDENS/DDPM}$ had no effect on fiber contractility

After verifying that our fluorescently labeled cTnC(T13C/N51C) constructs were efficiently incorporated into myocardial fibers, our next concern was whether the mutations inherent in cTnC(T13C/N51C), the presence of conjugated fluorophores, or extraction and reconstitution had disrupted thin filament regulation. Disruptive effects from these potential sources were ruled out by comparing normalized stress-Ca^{2+} relationships determined by Ca^{2+} titration of untreated (n = 5), CDTA treated (n = 5), cTnC(wt) reconstituted (n = 5), and $cTnC_{FRET}$ (n = 5) reconstituted fibers (Fig. 2b). Normalization was against the passive and maximal stress measured during the initial contraction. No appreciable deviations in contractility are visually evident in Fig. 2b. The average tension generating capacity, defined as the difference between maximal and passive stress, of the $cTnC_{FRET}$ reconstituted fiber group was ~91.5% ($p = 0.378$) that of the untreated fiber group (Table 1). Though this relative difference was not statistically significant, it was nevertheless consistent with the densitometry results from our SDS-PAGE and Western blot analysis (Fig. 1b). Importantly, there were no significant differences between pCa_{50} or n_H parameter values among the untreated, cTnC(wt) reconstituted, and $cTnC_{FRET}$ reconstituted fiber groups (Table 1). This indicated that our incorporation of $cTnC_{FRET}$ into myocardial fibers did not appreciably affect fiber contractility.

Ca^{2+}-dependent N-cTnC opening corresponded exactly with the force–Ca^{2+} relationship

The fact that reconstitution with $cTnC_{FRET}$ did not affect fiber contractility suggested that N-cTnC opening as monitored by AEDENS/DDPM FRET should be reflective of normal CRS conformational signaling in the relatively intact sarcomeres of detergent skinned fibers. This expectation was verified by the simultaneous measurement of fiber stress and fluorescence intensity during the Ca^{2+} titrations performed under normal XB cycling on the $cTnC_{FRET}$ reconstituted fiber group from Fig. 2b and a donor-only, $cTnC(T13C/N51C)_{AEDENS}$ reconstituted fiber group (n = 3) (Fig. 3a). The intensity from $cTnC_{FRET}$ fibers exhibited a sigmoidal dependence on Ca^{2+} level that is reminiscent of a typical stress–Ca^{2+} relationship and similar to what was observed in *in vitro* FRET studies [11,25,28], wherein Ca^{2+}-dependent N-cTnC opening also occurred sigmoidally but with a comparatively reduced steepness. Overall, *in situ* fluorescence intensity increased by a factor of 1.36 ± 0.08 when going from relaxing to maximally activating conditions. In contrast, the intensity observed from the $cTnC(T13C/N51C)_{AEDENS}$ fiber group was insensitive to changes in Ca^{2+} level, though the stress–Ca^{2+} relationship was no different than that for $cTnC_{FRET}$-reconstituted fibers (data not shown). In fact, a linear decrease in intensity with time (slope = −0.084 ABU·mm $^{-2}$·min, $R^2 = 0.8188$) was noted, the cause of which was likely photobleaching. Overall, these results indicated that the Ca^{2+}-dependent, sigmoidal increase in intensity from $cTnC_{FRET}$ fibers was due to changes in FRET caused by the opening of N-cTnC and the associated increase in the separation between Cys-13 and Cys-51.

Fluorescence intensity was normalized relative to the minimal and maximal fluorescence intensities observed during the initial contraction and fit with the Hill equation (Fig. 3b, Eqn. 1, $R^2 = 0.9998$). It is obvious that the relationship between Ca^{2+} and normalized *in situ* N-cTnC opening overlapped with the normalized stress–Ca^{2+} relationship. This was quantitatively confirmed by the best fit parameters obtained from nonlinear regression,

which are shown in Table 2. In comparing parameter values from Tables 1 and 2 for the $cTnC_{FRET}$ fiber group, no significant differences were obtained for pCa_{50} or n_H parameters ($p > 0.10$). This exact correspondence between *in situ* N-cTnC opening and fiber force development is strong biophysical evidence for a tight coupling between Ca^{2+}-induced thin filament activation and attachment of strong cycling XBs [50]. Such a tight coupling is consistent with the mechanism hypothesized to underlie positive feedback. The correspondence observed between stress and fluorescence is also notably consistent with observations by Sun *et al.*[31] using *in situ* fluorescence polarization that the Ca^{2+}-dependence of changes in N-cTnC C and E helix orientation overlapped with that of force generation. Therefore, our result in Fig. 3b indicated that the changes in α-helical orientation observed by Sun *et al.* were associated with N-cTnC opening.

Vanadate mediated inhibition of strong cross-bridge interactions reduced the overall exposure of the N-cTnC hydrophobic patch

Consistent with our hypothesis and the tight coupling observed between force generation and ensemble-averaged N-cTnC opening, we reasoned that inhibition of strong XB interactions with the thin filament should exert a destabilizing effect on the N-cTnC–cTnI-SR interaction. Therefore, inhibition should reduce the maximal extent of ensemble-averaged *in situ* hydrophobic patch exposure attributable to either the fraction of open N-cTnC molecules or the openness of the open N-cTnC conformation. This expectation was tested by performing Ca^{2+} titrations in the presence of 1 mM Vi on new groups of $cTnC_{FRET}$ ($n = 5$) and donor-only ($n = 3$) reconstituted fibers. Vi was chosen as the strong XB inhibitor for this experiment due its compatibility with the UV excitable AEDENS (in contrast with blebbistatin [51]) and its efficacy at disrupting the attachment of strong cycling XBs. It has been shown through *in situ* x-ray diffraction [52] that Vi-bound myosin heads are unable to move tropomyosin from the closed-state to open-state position. Furthermore, kinetic modeling [53] has indicated that Vi binding to strong XBs induces myosin detachment from actin and maintains myosin in a stable but inactive myosin•ADP•Vi complex. Though it was shown that the binding of myosin•ADP•Vi to actin can cause the release of ADP•Vi [54] and thereby reverse Vi-mediated inhibition [55], when Vi is concentrated enough it can presumably rebind to myosin such that inhibition is stably maintained [56]. Finally, appreciable Vi mediated UV photocleavage of myosin [43,44] under our experimental settings was not expected due to the presence of actin and ATP [46]; this expectation was verified by our Vi control experiments (see *Materials and Methods* section).

Fig. 4a shows traces of fluorescence intensity *vs.* pCa for Vi-treated fibers, and Fig. 4b shows the maximally inhibiting effect of 1 mM Vi on fiber force development. The intensity observed from Vi treated, donor-only $cTnC(T13C/N51C)_{AEDENS}$ fibers was insensitive to changes in Ca^{2+} level and unaffected by Vi treatment; photobleaching was again noted (linear decrease with slope = -0.065 ABUmm $^{-2}$·min, $R^2 = 0.9862$). In contrast, significant Vi-dependent effects were seen in the fluorescence intensity trace of $cTnC_{FRET}$ fibers. The maximal fluorescence intensity under maximally activating Ca^{2+} levels was significantly depressed, which implied a decreased ensemble-averaged separation between Cys-13 and Cys-51 of N-cTnC. This Vi-mediated depression in maximal ensemble-averaged N-cTnC opening was also observed when flushing the cuvette with Vi-containing activating solution (pCa = 4.3) immediately after an initial contraction in the absence of Vi (data not shown). N-cTnC opening became less sensitive to Ca^{2+} when Vi was present. These results collectively indicated that a reduction in the number of strong XB interactions had a destabilizing effect on the Ca^{2+}-sensitizing N-cTnC–cTnI-SR interaction. Interestingly, Vi appeared to leave the steepness of Ca^{2+}-induced N-cTnC opening relatively unaffected, indicating that cardiac thin filament cooperativity does not require the attachment of strong

XBs [8]. This was also consistent with the finding by Metzger [57] that cTnC plays an essential role in cardiac thin filament cooperativity.

The Hill equation (Eqn. 1) was very effective at describing normalized intensity (Fig. 4c) from Vi-treated $cTnC_{FRET}$ fibers ($R^2 = 0.9995$; see Table 2 for best fit parameters). Note that normalization was relative to the minimal and maximal fluorescence intensities observed during the initial contraction conducted in the absence of Vi. Under maximally activated conditions in the presence of Vi, the relative extent of hydrophobic patch exposure was only ~70% compared to the condition where XB cycling was present. This reduction in ensemble-averaged exposure could interpreted to indicate that the blocking of strong XBs reduced the steady-state fraction of open N-cTnC molecules, which assumes that the Ca^{2+}-saturated *in situ* thin filament is in a conformational equilibrium between blocked and closed states when strong XBs are absent [11,12]. We think that especially in the absence of strong XBs, such an equilibrium could result from a competitive balance between the drag-and-release mechanism [11] and the fly casting mechanism [24]; strong cycling XBs could thus be stabilizing the N-cTnC–cTnI-SR interaction by their disrupting effect on the fly casting mechanism [19]. However, the observed reduction in N-cTnC hydrophobic patch exposure could also be attributed to a weaker N-cTnC–cTnI-SR interaction [7], as that would reduce the openness and stability of the open conformation of N-cTnC. Either way, the observed effect of Vi treatment on N-cTnC opening indicated that interactions of strong cycling XBs with the thin filament stabilize the N-cTnC–cTnI-SR interaction such that ensemble-averaged exposure of the N-cTnC hydrophobic patch is increased by at least 1.4 fold. Furthermore, this conformational stabilization effect was correlated with a significant increase in pCa_{50} from 5.66 in the absence of strong cycling XBs to 5.92 in their presence ($p < 0.0001$), a result consistent with our hypothesis.

Nonlinear regression confirmed that Vi-mediated depression of N-cTnC opening had no discernible effect on thin filament cooperativity. Though there was a small decrease in the Hill coefficient relative to conditions of normal XB cycling, this decrease was not statistically significant ($p = 0.5441$). Since N-cTnC opening is diagnostic of the blocked-state to closed-state transition, this indicated that Ca^{2+} was able to cooperatively bind and switch the thin filament on even though the positive feedback mechanism was blocked. This implied that the primary biophysical role of the positive feedback mechanism is to adjust the Ca^{2+}-sensitivity of CRS signaling and stabilize activation, rather than to render it a cooperative process. Our results thus implicated the positive feedback mechanism as responsible for the hysteresis, and not cooperativity, of Ca^{2+} binding. This conclusion is supported by recent evidence [8,27,31,33] that thin filament cooperativity does not require strong XB interactions, and instead primarily depends upon the organization and coupling of protein-protein interactions that is inherent in thin filament ultrastructure.

Non-cycling strong cross-bridges stimulated partial ensemble-averaged N-cTnC-opening under nanomolar, resting Ca^{2+} levels

Since inhibition of strong XB connections with the thin filament had a destabilizing effect on the N-cTnC–cTnI-SR interaction, we thought that a maximum interaction between non-cycling strong XBs and the thin filament should produce a considerable stabilizing effect. The Ca^{2+}-independent movement of tropomyosin from the blocked-state to open-state position by the strong binding of myosin should reposition cTnI on actin and promote interaction between N-cTnC and cTnI-SR [11,19]. This expectation was tested by replacing ATP with ADP in Ca^{2+} titrations performed on new groups of $cTnC_{FRET}$ ($n = 5$) and donor-only ($n = 3$) reconstituted fibers (Fig. 5). Such Ca^{2+} titrations essentially represent the stimulation of Ca^{2+}-dependent thin filament activation starting from the recently proposed "Open minus Ca^{2+}" pre-relax state of thin filament regulation [5] rather than the blocked-state. The strongly binding myosin•ADP state was chosen instead of the rigor myosin state

because the myosin•ADP state is more consistent with our prior *in vitro* biophysical studies that have used S1•ADP [11]. Furthermore, it is known that the strong binding of myosin to actin, and not the nucleotide state of myosin, is the primary determinant in the closed-state to open-state transition [58].

The flushing of HR+ADP (wherein ATP had been replaced with ADP) into the cuvette immediately led to Ca^{2+}-independent, maximal generation of force (Fig. 5a). This confirmed that our protocol led to a maximum interaction of non-cycling strong XBs with thin filaments and suggested that the pre-relax state of thin filament regulation had been induced. Interestingly, ADP treatment also led to a significant but submaximal increase in fluorescence intensity (Fig. 5a). The fluorescence intensity increased from its basal value to ~30% of what was observed during the initial contraction that had been conducted under normal conditions. As expected, this indicated that in the pre-relax state [5] the Ca^{2+} independent, strong XB induced movement of tropomyosin from the blocked-state to the open-state position had a significant stabilizing effect on the open conformation of N-cTnC by promoting the N-cTnC–cTnI-SR interaction. Interestingly, the resultant partial ensemble-averaged opening of N-cTnC is suggestive of a strong XB induced conformational equilibrium between closed and open N-cTnC conformations; this would be similar to the conformational equilibrium stimulated by Ca^{2+} binding [22].

Both Ca^{2+} and strong myosin binding are required to achieve maximal N-cTnC opening *in vitro*[28], and Ca^{2+} titrations demonstrated that this is also the case *in situ*. Fig. 5c shows traces of fluorescence intensity *versus* pCa for ADP-treated fibers, and Fig. 5b shows that 5 mM ADP•Mg led to maximal fiber stress throughout the Ca^{2+} titration. The intensity observed from ADP-treated, donor-only $cTnC(T13C/N51C)_{AEDENS}$ fibers was insensitive to changes in Ca^{2+} level, unaffected by the replacement of ATP with ADP, and found to exhibit a linear decrease with time from photobleaching (slope = −0.107 ABU·mm $^{-2}$·min, $R^2 = 0.9553$). In contrast, FRET measurements indicated that ADP treatment caused additional, Ca^{2+}-induced N-cTnC opening to begin occurring at much lower Ca^{2+} levels (pCa of ~7.5 *versus* ~6.5 in the absence of ADP) and to respond less steeply and more sensitively to increasing Ca^{2+}. However, the maximal extent of ensemble-averaged N-cTnC opening under saturating Ca^{2+} levels for ADP-treated fibers appeared to be the same as for untreated fibers.

Fig. 5d shows the intensity trace for ADP-treated $cTnC_{FRET}$ fibers as normalized and fit with the Hill equation (Eqn. 1, $R^2 = 0.9999$, best fit parameters shown in Table 2). ADP treatment caused no significant difference in maximal normalized fluorescence, but significantly increased both the starting fluorescence intensity and pCa_{50} and significantly decreased n_H to a value of ~1. The stabilizing effect of non-cycling strong XBs on the N-cTnC–cTnI-SR interaction, as implied by FRET, thus produced a significant ~6-fold Ca^{2+}-sensitization of CRS signaling compared to the case where strong XB interactions were blocked by Vi. This was consistent with our hypothesis and the expected behavior of the fourth, pre-relax state of thin filament regulation [5]. The fact that thin filament cooperativity was attenuated by ADP treatment also implies that cooperativity requires the Ca^{2+}-dependent movement of tropomyosin, which was retarded by virtue of it being locked in the open-state position by myosin in the A-band of the myofilament lattice.

Along these lines, the positive feedback mechanism should be expected to predominately affect the A-band, which takes up approximately 蔻 of the sarcomere at a sarcomere length of 2.3 μm. This point was astutely made by Sun *et al.*[31] and led them to propose the two Hill equation model encapsulated in Eqn. 2; therefore, we also fit Eqn. 2 to our FRET data from Fig. 5d ($R^2 = 0.9999$). Best fit parameters obtained from nonlinear regression were $\alpha = 0.59$, $\theta_{min} = 0.308 \pm 0.059$, $\theta_{max} = 1.010 \pm 0.026$, $n_{H,A} = 1.31 \pm 0.80$, $pCa_{50,A} = 6.88 \pm 0.23$,

$n_{H,I}$ = 1.94 ± 1.12, $pCa_{50,I}$ = 5.86 ± 0.32. The values of α and pCa_{50},A were thus consistent with the Ca^{2+}-sensitizing effect expected for positive feedback from non-cycling strong XBs having significantly Ca^{2+}-sensitized cTn molecules located in the A-band. Furthermore, the values of $n_{H,I}$, and $pCa_{50,I}$ were consistent with the positive feedback mechanism having not affected cTn molecules found in the I-band; $n_{H,I}$ and $pCa_{50,I}$ were not significantly different from the n_H and pCa_{50} obtained under conditions of inhibited XB cycling (p = 0.1076 and 0.2047, respectively). Therefore, both the positive feedback mechanism and the pre-relax state were implicated by FRET as being confined to the A-band. Though $n_{H,I}$ was not significantly different from $n_{H,A}$ (p = 0.3360), it was clear that $n_{H,A}$ was more significantly less than n_H obtained under conditions of inhibited XB cycling (p = 0.0089) than $n_{H,I}$. This implied that non-cycling strong XB interactions had actually attenuated the cooperativity of Ca^{2+}-dependent thin filament activation in the A-band. Finally, comparison of $pCa_{50,A}$ with $pCa_{50,I}$ suggested that the positive feedback mechanism is capable of sensitizing cTnC to Ca^{2+} by up to ∼10-fold, which more than accounts for the fold Ca^{2+}-sensitization implied in the hysteresis of the force–Ca^{2+} relationship [30].

As for the validity of Eqn. 2 as a descriptive model of our FRET data, AIC values (Eqn. 3) were used to compare the models represented in Eqn. 1 and Eqn. 2. AIC values of −14.82 and −33.24 (Eqn. 3) were obtained for the fits of Eqns. 1 and 2, respectively, to the data in Fig. 5d; this indicated that Eqn. 2 was 9,990 times better (Eqn. 4) at describing our ADP-treated FRET data. That Eqn. 2 is a better model is also visually evident from Fig. 5d. Therefore, it was concluded that our FRET data not only strongly supported the hypothesized biophysical basis for the positive feedback mechanism in cardiac muscle, but also showed that the mechanism occurs in the sarcomere where it should: that is, exactly where strong cycling XBs are able to interact with the thin filament. This also implies that the pre-relax state of thin filament regulation [5], now being mechanistically attributed to the positive feedback mechanism as characterized in this study, is confined to the A-band. Based on these results, we also attempted to fit Eqn. 2 to the FRET data from untreated $cTnC_{FRET}$ reconstituted fibers. When accounting for the fact that the overall extent of Ca^{2+} triggered N-cTnC opening in the A-band should be ∼1.4 fold greater than in the I-band under normal XB cycling, the best fit was obtained with α = 0.021, wherein $n_{H,I}$ = 3.65 ± 0.53 and $pCa_{50,I}$ = 5.90 ± 0.02 (*i.e.* parameter values not significantly different from those obtained by Eqn. 1). This implied that the model represented by Eqn. 2 could no longer distinguish the A-band from the I-band under conditions of normal XB cycling. This indicated that the strong interactions of cycling XBs with the thin filament were able to confer positive feedback in the A-band without the disruptive effect on thin filament cooperativity that was observed for non-cycling strong XB interactions.

Discussion

Through the use of steady-state FRET to monitor the *in situ* conformational behavior of N-cTnC opening, it has been biophysically demonstrated that the stabilizing effect of strong XB interactions on the Ca^{2+}-sensitizing N-cTnC–cTnI-SR interaction serves as the structural basis for the positive feedback mechanism. This study thus points to a central role for the N-cTnC–cTnI-SR interaction in physiological thin filament regulation. It is implied by our FRET data that the positive feedback mechanism would not be possible without the stabilizing effect of cTnI-SR on the open conformation of N-cTnC. Accordingly, it is now clear that in the molecular environment of the myofilament lattice, cTnI-SR opens N-cTnC, stabilizes Ca^{2+}-binding, triggers activation, translates positive feedback from strong XB interactions into Ca^{2+}-sensitization, plays an essential role in the fourth pre-relax state of thin filament regulation, and is centrally involved in creating the hysteresis of Ca^{2+} binding. However, this study also points to a central role for myosin in physiological thin filament regulation due to its ability to stabilize the N-cTnC–cTnI-Sr interaction through structural

feedback from strong XB interactions. Due to the nature of our FRET data, it is possible that this stabilization could enable a greater proportion of the N-cTnC molecular population to interact with cTnI-SR (Fig. 6a part i) [11,12], or it could tighten the N-cTnC–cTnI-SR interaction itself (Fig. 6a part ii). Regardless, it is clear that both Ca^{2+} and myosin are not only needed to fully stabilize thin filament activation, but also to achieve the interconnected molecular mechanisms that underlie the efficient regulatory response of the thin filament to Ca^{2+} signals.

The collective structural interpretation of our biophysical results is depicted in Fig. 6b-c. The main determinant of CRS Ca^{2+} sensitivity was implicated by FRET to be the overall stability of the *in situ* open conformation of N-cTnC (Fig. 6b). The essence of the positive feedback mechanism is that many factors can contribute to this stability in the cardiac sarcomere, especially strong XB interactions. The implications for the four states [5] of thin filament regulation are as follows (Fig. 6c). In the absence of Ca^{2+} (Fig. 6c part i), the thin filament is in the blocked state and N-cTnC is in a closed conformation wherein the hydrophobic patch is buried. In the presence of saturating Ca^{2+} (Fig. 6c part ii), the binding of Ca^{2+} to N-cTnC has stimulated the opening of N-cTnC [22] and the N-cTnC–cTnI-SR interaction. The thin filament has thus entered the closed state *via* the drag-and-release mechanism [11,19]. However, the stability of the N-cTnC–cTnI-SR interaction is most likely constrained by the interactions between cTnI-MD and actin that are related to the fly casting mechanism [13,19,24]. Therefore, the thin filament may be in a conformational equilibrium between blocked and closed states [11,12], or the openness of the open conformation of N-cTnC may be reduced. In the absence of Ca^{2+} and presence of strong XB interactions with the thin filament (Fig. 6c part iii), strong XBs have moved Tm from the blocked-state to open-state position and have fully disrupted the interactions between actin and cTnI-IR and cTnI-MD [13,19]. The release of these constraints on cTnI-SR allows it to stimulate a Ca^{2+}-sensitized, partial opening of N-cTnC, and the thin filament thus enters the pre-relax state [5]. It is possible that this partial opening represents a significantly weakened N-cTnC–cTnI-SR interaction wherein the hydrophobic patch is truly partially exposed. However, based on the recent *in vitro* EPR work of Cordina *et al.*[22] and our prior *in vitro* FRET studies [11,12], we think that a more likely possibility is “inverted” conformational selection. In this mechanism, the cTnI-SR–N-cTnC interaction would be destabilized in the absence of Ca^{2+} such that N-cTnC would be in a conformational equilibrium between its closed and open conformations; and Ca^{2+}, rather than cTnI-SR, would then conformationally select the open conformation. Finally, in the presence of saturating Ca^{2+} and strong XB interactions (Fig. 6c part iv), strong XBs have shifted at least the A-band thin filament into the open state. The movement of tropomyosin to the open-state position has fully disrupted the conformational constraints on cTnI-SR, producing a fully stabilized N-cTnC–cTnI-SR interaction and maximum Ca^{2+}-sensitization. Overall, the positive feedback mechanism is required to fully activate the TF, and thereby fully stabilize the N-cTnC–cTnI-SR interaction and the open conformation of N-cTnC.

Our results also have important implications for understanding cardiac thin filament cooperativity. Our FRET data clearly indicated that the entire thin filament cooperatively switches on just as steeply even in the complete absence of strong XB interactions. Furthermore, though the positive feedback mechanism was confined to the A-band, we nevertheless observed cooperative thin filament activation occurring in the I-band. These results are supported by other recent lines of biophysical evidence [27,31] and the finding of Metzger [57] that partial TnC extraction depresses n_H especially in cardiac muscle. However, our FRET data complicates the picture of what an “activated” physiological thin filament could mean by suggesting the possibility of a conformational equilibrium between blocked and closed states in the absence of strong XBs. We speculated that such an equilibrium could result from a competitive balance between the drag-and-release

mechanism [11] and the fly casting mechanism [24]. Therefore, thin filament cooperativity could involve a cooperative spread of changes in conformational equilibria along the thin filament [12]. In any case, out of the possible mechanisms that could determine n_H in cardiac muscle [32], our FRET data strongly suggested that neither regulatory-unit–XB interactions nor XB–XB interactions play an essential role. Interactions between regulatory units, the movement of tropomyosin, and the properties of cTn and tropomyosin were instead implicated as being critically involved in determining n_H. However, our results also imply that strong cycling XBs are able to significantly sensitize the A-band to Ca^{2+} without disrupting thin filament cooperativity. Therefore, though the positive feedback mechanism is not essential to cardiac thin filament cooperativity, and may even disrupt cooperativity during ischemia [8,33], it nonetheless works compatibly with cooperativity under physiological conditions.

Though positive feedback did not appear to play a dominant role in the mechanism underlying thin filament cooperativity, our study implicated strong XB mediated stabilization of the N-cTnC–cTnI-SR interaction as explaining another important aspect of normal physiological myocardial behavior: Ca^{2+} binding hysteresis [29,30]. Our FRET data clearly showed that the open conformation of N-cTnC is stabilized by the presence of strong XB interactions. Therefore, less free Ca^{2+} should be required to sustain thin filament activation than to stimulate it. Interestingly, this is exactly what is observed in myocardial dynamics; the relatively fast Ca^{2+} transient of a typical cardiomyocyte leads the relatively slow and delayed force transient [8]. Sarcomeric free [Ca^{2+}] can rise to near peak levels before force even begins to respond, and [Ca^{2+}] can decrease to half of the peak level before twitch force even begins to decrease. These phenomena are consistent with a Ca^{2+} hysteresis caused by the positive feedback mechanism as biophysically characterized in this study. Based on our findings, there should be a requirement that Ca^{2+} levels accumulate significantly to stimulate the blocked-state to closed-state transition. Once this occurs, strong XB connections should begin, which should stimulate the closed-state to open-state transition. The concurrent strong XB mediated stabilization of the N-cTnC–cTnI-SR interaction should then enhance the Ca^{2+} affinity of N-cTnC such that less free Ca^{2+} is needed in the sarcomere to sustain the Ca^{2+} bound state and thus the twitch. This should enable the cardiomyocyte to begin removing Ca^{2+} from the sarcomere well before the twitch is complete [8]. This analysis suggests that the positive feedback mechanism thereby plays an important role in promoting tight and efficient control of Ca^{2+} fluxes and Ca^{2+} response through a mechanism made possible by the ability of strong XB interactions with the thin filament to modulate the stability of the open N-cTnC conformation.

Clearly, the evolutionary purpose of myosin motors is not solelyito generate force, but also to stabilize thin filament activation and adjust the Ca^{2+}-affinity of N-cTnC by an elegantly balanced and impressively allosteric mechanism. This FRET study thus supports the idea that there is considerable therapeutic potential in the ability of myosin to sensitize the thin filament to Ca^{2+}[8]. However, much remains to be determined about the role of positive feedback in the dynamic, time-varying behavior of the myocardial sarcomere. In the future, it will be especially interesting, and important, to characterize the *in situ* kinetics and dynamics [8] of the structural basis for the positive feedback mechanism that this steady-state biophysical study provides. It will also be important to biophysically determine how the positive feedback mechanism is related to other mechanisms that impact the stability of the open N-cTnC conformation, such as the conformational effects of PKA signaling [59] and the Frank-Starling mechanism [32]. Finally, more evidence is needed to establish whether the stabilizing effect of strong XBs on the N-cTnC–cTnI-SR interaction represents a shift in conformational equilibrium or a modified open N-cTnC conformation.

Acknowledgments

We would like to thank John Robinson and Murali Chandra for accomplishing the initial setup of the Muscle Research System for experimental use. We thank Danuta Szczesna-Cordary for the generous gift of wild type myosin regulatory light chain from rat that was used in our cTnC extraction and replacement protocol. We would also like to further express our gratitude to Murali Chandra for helpful discussions about the project and the manuscript. We also thank Steven Ford for helpful discussions concerning analysis of model effectiveness. Finally, this work was supported, in whole or in part, by National Institutes of Health Grants R01 HL80186-5S1 (to W.-J. D.) and R01 HL64035 (to R.J.S.), and also the M. J. Murdock Charitable Trust (to W.-J. D.). The study described in this manuscript was also supported by Award Number T32GM008336 from the NIGMS. The content is solely the responsibility of the authors and does not necessarily represent the official views of the National Institute of General Medical Sciences or the National Institutes of Health.

References

1. Bremel RD, Weber A. Nat New Biol. 1972; 238:97–101. [PubMed: 4261616]
2. Pan BS, Solaro RJ. J Biol Chem. 1987; 262:7839–7849. [PubMed: 3584144]
3. Allen DG, Kentish JC. J Physiol. 1988; 407:489–503. [PubMed: 3151492]
4. Moss RL, Razumova M, Fitzsimons DP. Circ Res. 2004; 94:1290–1300. [PubMed: 15166116]
5. Lehrer SS. J Muscle Res Cell Motil. 2011; 32:203–208. [PubMed: 21948173]
6. Hinken AC, Solaro RJ. Physiology (Bethesda). 2007; 22:73–80. [PubMed: 17420299]
7. Gillis TE, Martyn DA, Rivera AJ, Regnier M. J Physiol. 2007; 580:561–576. [PubMed: 17317743]
8. Solaro RJ. J Biomed Biotechnol. 2010; 2010:105648. [PubMed: 20467475]
9. Gordon AM, Homsher E, Regnier M. Physiol Rev. 2000; 80:853–924. [PubMed: 10747208]
10. Kobayashi T, Solaro RJ. Annu Rev Physiol. 2005; 67:39–67. [PubMed: 15709952]
11. Robinson JM, Dong WJ, Xing J, Cheung HC. J Mol Biol. 2004; 340:295–305. [PubMed: 15201053]
12. Robinson JM, Cheung HC, Dong W. Biophys J. 2008; 95:4772–4789. [PubMed: 18676638]
13. Galińska A, Hatch V, Craig R, Murphy AM, Van Eyk JE, Wang CL, Lehman W, Foster DB. Circ Res. 2010; 106:705–711. [PubMed: 20035081]
14. Vibert P, Craig R, Lehman W. J Mol Biol. 1997; 266:8–14. [PubMed: 9054965]
15. Li MX, Wang X, Sykes BD. J Muscle Res Cell Motil. 2004; 25:559–579. [PubMed: 15711886]
16. Galińska-Rakoczy A, Engel P, Xu C, Jung H, Craig R, Tobacman LS, Lehman W. J Mol Biol. 2008; 379:929–935. [PubMed: 18514658]
17. McKillop DF, Geeves MA. Biophys J. 1993; 65:693–701. [PubMed: 8218897]
18. Craig R, Lehman W. J Mol Biol. 2001; 311:1027–1036. [PubMed: 11531337]
19. Zhou Z, Li KL, Rieck D, Ouyang Y, Chandra M, Dong WJ. J Biol Chem. 2012; 287:7661–7674. [PubMed: 22207765]
20. Li MX, Spyracopoulos L, Sykes BD. Biochemistry. 1999; 38:8289–8298. [PubMed: 10387074]
21. Dong WJ, Xing J, Villain M, Hellinger M, Robinson JM, Chandra M, Solaro RJ, Umeda PK, Cheung HC. J Biol Chem. 1999; 274:31382–31390. [PubMed: 10531339]
22. Cordina NM, Liew CK, Gell DA, Fajer PG, Mackay JP, Brown LJ. Biochemistry. 2013; 52:1950–1962. [PubMed: 23425245]
23. Xing J, Chinnaraj M, Zhang Z, Cheung HC, Dong WJ. Biochemistry. 2008; 47:13383–13393. [PubMed: 19053249]
24. Hoffman RM, Blumenschein TM, Sykes BD. J Mol Biol. 2006; 361:625–633. [PubMed: 16876196]
25. Xing J, Jayasundar JJ, Ouyang Y, Dong WJ. J Biol Chem. 2009; 284:16432–16441. [PubMed: 19369252]
26. Zhou Z, Rieck D, Li KL, Ouyang Y, Dong WJ. Arch Biochem Biophys. 2013; 535:56–67. [PubMed: 23246786]
27. Davis JP, Norman C, Kobayashi T, Solaro RJ, Swartz DR, Tikunova SB. Biophys J. 2007; 92:3195–3206. [PubMed: 17293397]

28. Dong WJ, Jayasundar JJ, An J, Xing J, Cheung HC. Biochemistry. 2007; 46:9752–9761. [PubMed: 17676764]
29. Ridgway EB, Gordon AM, Martyn DA. Science. 1983; 219:1075–1077. [PubMed: 6823567]
30. Harrison SM, Lamont C, Miller DJ. J Physiol. 1988; 401:115–143. [PubMed: 3171985]
31. Sun YB, Lou F, Irving M. J Physiol. 2009; 587:155–163. [PubMed: 19015190]
32. Smith L, Tainter C, Regnier M, Martyn DA. Biophys J. 2009; 96:3692–3702. [PubMed: 19413974]
33. Solaro RJ. J Physiol. 2009; 587:3. [PubMed: 19119179]
34. Sun YB, Irving M. J Mol Cell Cardiol. 2010; 48:859–865. [PubMed: 20004664]
35. Gaponenko V, Abusamhadneh E, Abbott MB, Finley N, Gasmi-Seabrook G, Solaro RJ, Rance M, Rosevear PR. J Biol Chem. 1999; 274:16681–16684. [PubMed: 10358006]
36. Dweck D, Reyes-Alfonso A Jr, Potter JD. Anal Biochem. 2005; 347:303–315. [PubMed: 16289079]
37. Chandra M, Tschirgi ML, Ford SJ, Slinker BK, Campbell KB. Am J Physiol Regul Integr Comp Physiol. 2007; 293:R1595–1607. [PubMed: 17626127]
38. Fujita H, Sasaki D, Fukuda K, Ishiwata S. J Physiol. 2002; 542:221–229. [PubMed: 12096063]
39. Szczesna-Cordary D, Guzman G, Ng SS, Zhao J. J Biol Chem. 2004; 279:3535–3542. [PubMed: 14594949]
40. Allen K, Xu YY, Kerrick WG. J Appl Physiol. 2000; 88:180–185. [PubMed: 10642379]
41. Guth K, Junge J. Nature. 1982; 300:775–776. [PubMed: 6217425]
42. Strauss JD, Zeugner C, Van Eyk JE, Bletz C, Troschka M, Ruegg JC. FEBS Lett. 1992; 310:229–234. [PubMed: 1397278]
43. Grammer JC, Cremo CR, Yount RG. Biochemistry. 1988; 27:8408–8415. [PubMed: 2977286]
44. Mocz G. Eur J Biochem. 1989; 179:373–378. [PubMed: 2537208]
45. Cremo CR, Long GT, Grammer JC. Biochemistry. 1990; 29:7982–7990. [PubMed: 2261455]
46. Muhlrad A, Peyser YM, Ringel I. Biochemistry. 1991; 30:958–965. [PubMed: 1824926]
47. Akaike H. IEEE Transactions on Automatic Control. 1974; 19:716–723.
48. Burnham KP, Anderson DR. Sociological Methods & Research. 2004; 33:261–304.
49. Akaike H. Journal of Econometrics. 1981; 16:3–14.
50. Fukuda N, Terui T, Ohtsuki I, Ishiwata S, Kurihara S. Curr Cardiol Rev. 2009; 5:119–124. [PubMed: 20436852]
51. Sakamoto T, Limouze J, Combs CA, Straight AF, Sellers JR. Biochemistry. 2005; 44:584–588. [PubMed: 15641783]
52. Bekyarova TI, Reedy MC, Baumann BA, Tregear RT, Ward A, Krzic U, Prince KM, Perz-Edwards RJ, Reconditi M, Gore D, Irving TC, Reedy MK. Proc Natl Acad Sci U S A. 2008; 105:10372–10377. [PubMed: 18658238]
53. Caremani M, Lehman S, Lombardi V, Linari M. Biophys J. 2011; 100:665–674. [PubMed: 21281581]
54. Werber MM, Peyser YM, Muhlrad A. Biochemistry. 1992; 31:7190–7197. [PubMed: 1386527]
55. Prochniewicz E, Walseth TF, Thomas DD. Biochemistry. 2004; 43:10642–10652. [PubMed: 15311925]
56. Xu J, Root DD. Biophys J. 2000; 79:1498–1510. [PubMed: 10969011]
57. Metzger JM. Biophys J. 1995; 68:1430–1442. [PubMed: 7787029]
58. Zhang D, Yancey KW, Swartz DR. Biophys J. 2000; 78:3103–3111. [PubMed: 10827987]
59. Sadayappan S, Finley N, Howarth JW, Osinska H, Klevitsky R, Lorenz JN, Rosevear PR, Robbins J. FASEB J. 2008; 22:1246–1257. [PubMed: 17984178]
60. Spyracopoulos L, Li MX, Sia SK, Gagne SM, Chandra M, Solaro RJ, Sykes BD. Biochemistry. 1997; 36:12138–12146. [PubMed: 9315850]
61. Schrödinger L. The PyMOL Molecular Graphics System, Version 1.1r1. 2008

Abbreviations used

BDM	2,3-butanedione monoxime
CRS	Ca^{2+}-sensitive regulatory switch
cTn	cardiac troponin
DDPM	N-(4-dimethylamino-3,5-dinitrophenyl)maleimide
$cTnC_{FRET}$	$cTnC(T13C/N51C)_{AEDENS/DDPM}$
FRET	Förster resonance energy transfer
IAEDENS	5-(iodoacetamidoethyl)aminonaphthelene-1-sulfonic acid
HR	highly relaxing
Ir	inhibitory region
Md	mobile domain
N-cTnC	N-domain of cTnC
PI	protease inhibitors
Sr	switch region
Vi	orthovanadate
XB	cross-bridge

Highlights

FRET was used to monitor Ca^{2+}-dependent N-cTnC opening in skinned myocardial fibers Inhibition of strong cross-bridges reduced the maximal extent of N-cTnC opening Cycling cross-bridges enhanced the overall exposure of the N-cTnC hydrophobic patch Non-cycling strong cross-bridges stimulated N-cTnC opening under nanomolar Ca^{2+} The overall stability of N-cTnC opening correlated positively with Ca^{2+} sensitivity

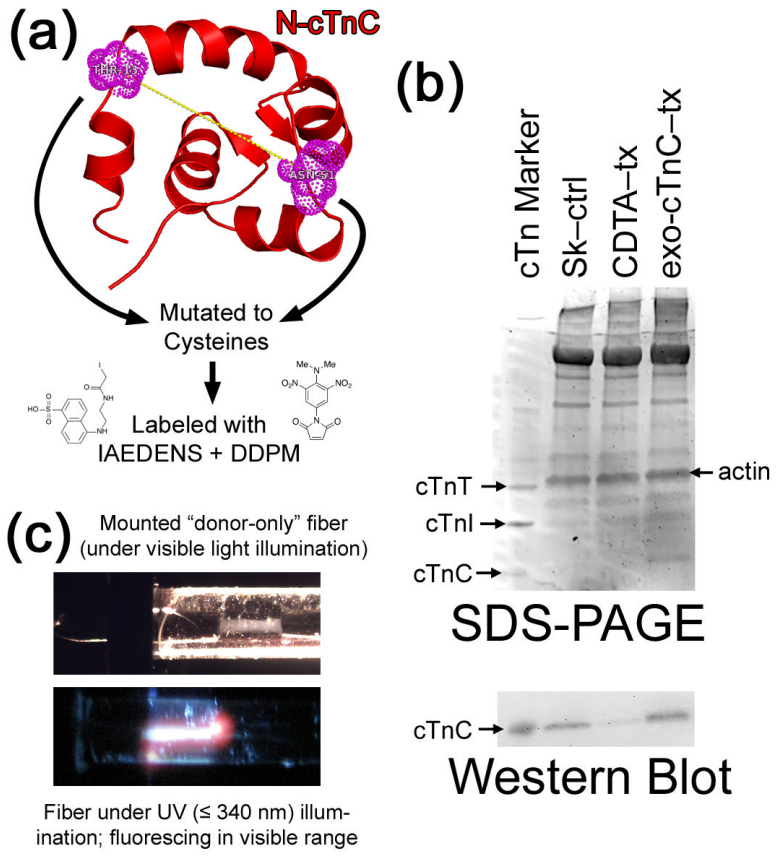

Figure 1.

The results of CDTA-mediated extraction of endogenous N-cTnC from detergent skinned fibers and reconstitution with fluorescently labeled cTnC(T13C/N51C) constructs. (a) This schematic depicts our use of FRET to sense ensemble-averaged *in situ* N-cTnC opening. N-cTnC is visualized from PDB structure 1AP4 [60] using PyMOL [61]. Thr-13 and Asn-51 (highlighted by magenta colored dot clouds) are located N-terminal to the first E-F hand moiety and between the first and second E-F hand moieties of N-cTnC, respectively. After labeling, the AEDENS/DDPM FRET pair is thus ideally positioned to sense the ensemble-averaged extent of N-cTnC hydrophobic patch exposure. (b) Samples of skinned fibers (Sk–ctrl, n = 6), skinned fibers treated with CDTA (CDTA–tx, n = 6), and CDTA-treated fibers further treated with exogenous $cTnC_{FRET}$ (exo-cTnC–tx, n = 6) were loaded into the 15% SDS-PAGE gel shown. Densitometric analysis of the actin bands determined that protein loading was 120% and 113% in CDTA–tx and exo-cTnC–tx lanes, respectively, relative to the Sk–ctrl lane. Analysis of the subsequent Western blot determined that ~85% of the endogenous cTnC was removed by CDTA treatment, and ~93% of the removed cTnC was replaced with $cTnC_{FRET}$. C) Visible light photographs show the expected emission of violet/blue visible light from a mounted, donor-only $cTnC(T13C/N51C)_{AEDENS}$ reconstituted fiber when under excitatory illumination by UV light.

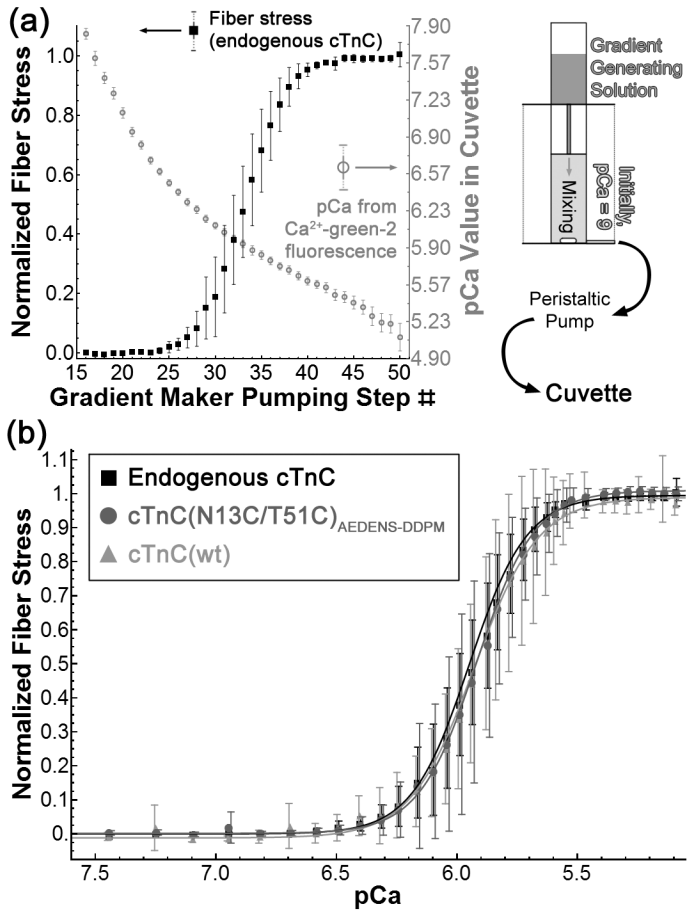

Figure 2.

A comparison of the steady-state, isometric (sarcomere length = 2.3 μm) force–Ca^{2+} relationships of untreated skinned fibers (n = 5), skinned fibers reconstituted with $cTnC_{FRET}$ (n = 5), and fibers reconstituted with cTnC(wt) (n = 5). (a) The stress–Ca^{2+} relationship of untreated skinned fibers is shown alongside cuvette pCa value (n = 3 trials) as a function of gradient maker pumping step. Cuvette pCa values were calculated from measurements of Ca^{2+}-green-2 fluorescence using the approach of Allen *et al.*[40]. (b) Normalized, average stress values ± SD *versus* cuvette pCa value are plotted alongside fits of the Hill equation to each data set. Each trace was normalized relative to the maximal (pCa = 4.3) and minimal (pCa = 9) average stress values observed for the data set. Best-fit Hill equation parameters are given in Table 1.

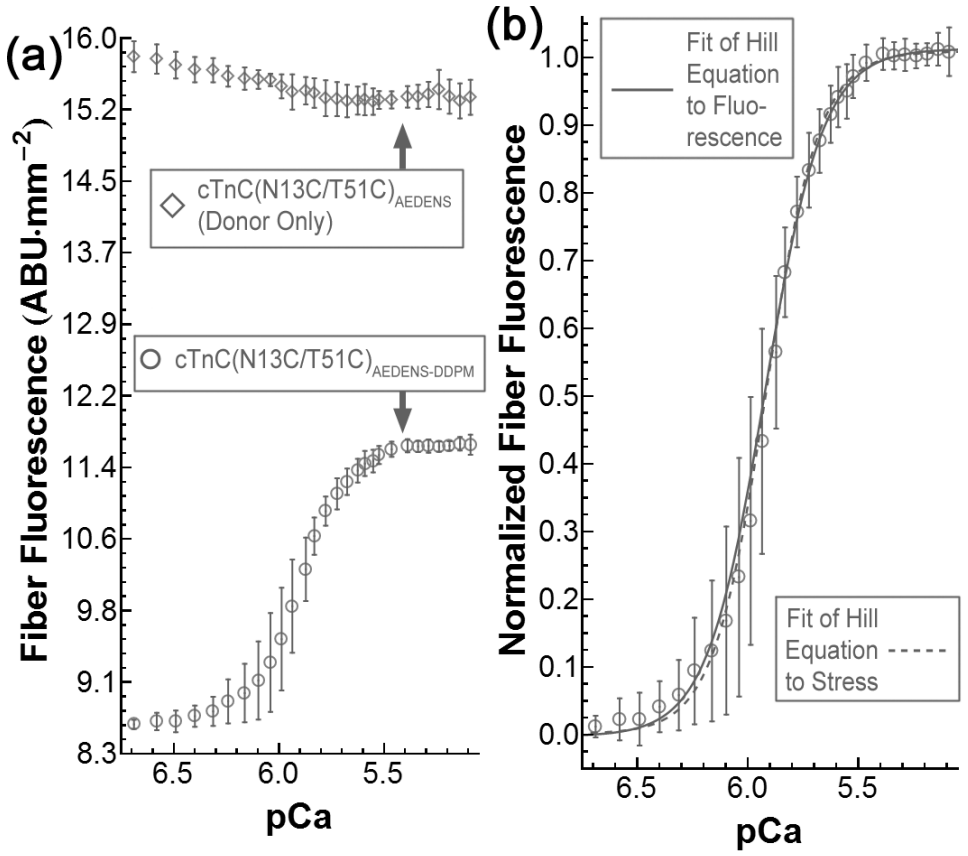

Figure 3.

Use of FRET to measure the *in situ*, steady-state Ca^{2+}-dependence of ensemble-averaged N-cTnC opening under conditions of normal XB cycling in fibers reconstituted with fluorescently labeled cTnC constructs. (a) Fiber fluorescence as a function of pCa observed for fibers reconstituted with $cTnC_{FRET}$ (n = 5, same set of fibers as appears in Fig. 2b) and donor-only $cTnC(T13C/N51C)_{AEDENS}$ (n = 3). Fiber fluorescence intensity is defined here as emission intensity per fiber cross sectional area, and is thus a fluorescence analog of fiber stress. (b) Fiber fluorescence data from the $cTnC_{FRET}$ reconstituted fibers of panel (a) now normalized and fit with the Hill equation. Normalization was relative to the maximal (pCa = 4.3) and minimal (pCa = 9) average fiber fluorescence intensity values of the data set. The Hill equation fit to fiber stress data from Fig. 2b is shown for comparison as a faded, light gray trace.

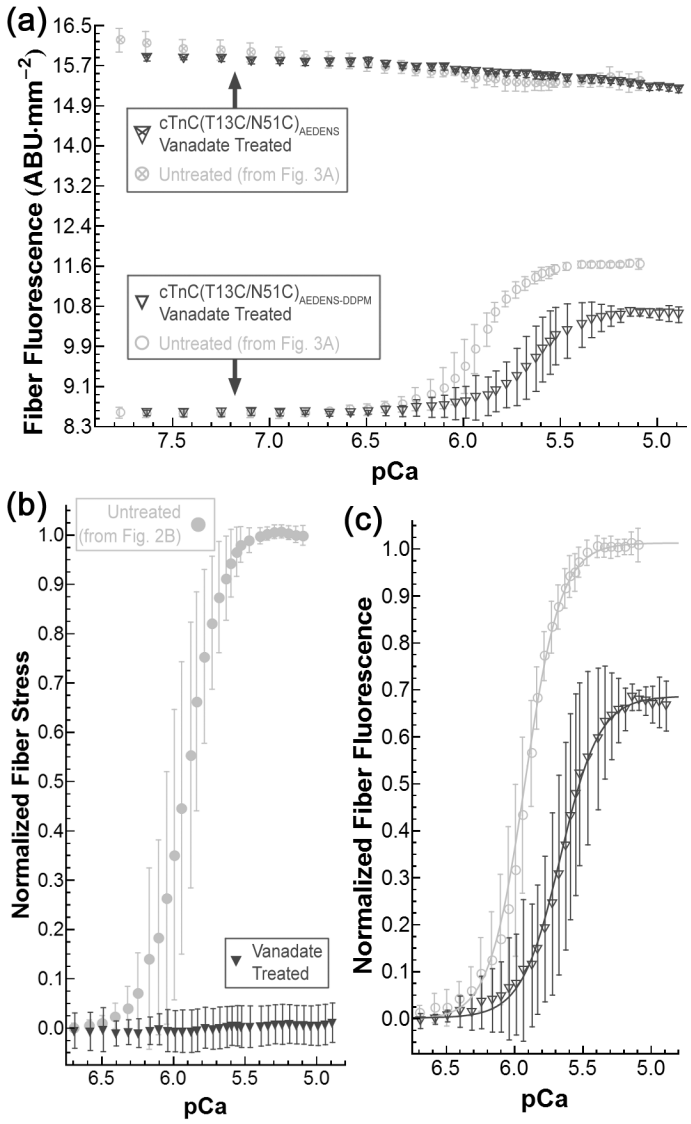

Figure 4.

Application of FRET to determine the effects of Vi-mediated inhibition of strong XB interactions on the Ca^{2+}-dependent exposure of the N-cTnC hydrophobic patch. (a) Fiber fluorescence intensity as a function of pCa observed for fibers perfused with increasing levels of Ca^{2+} in the presence of 1 mM Vi and reconstituted with either $cTnC_{FRET}$ (n = 5) or donor-only $cTnC(T13C/N51C)_{AEDENS}$ (n = 3) (dark gray traces). Fiber fluorescence intensity data from Fig. 3a has been included for comparison (light gray traces). (b) Stress as a function of pCa observed for the Vi treated, $cTnC_{FRET}$ reconstituted fibers from panel (a). (c) Fiber fluorescence intensity data from panel (a) now normalized and fit with the Hill equation. Normalization was relative to the maximal (pCa = 4.3) and minimal (pCa = 9) average intensity values observed during initial contractions conducted in the absence of Vi. Best-fit Hill equation parameters are given in Table 2.

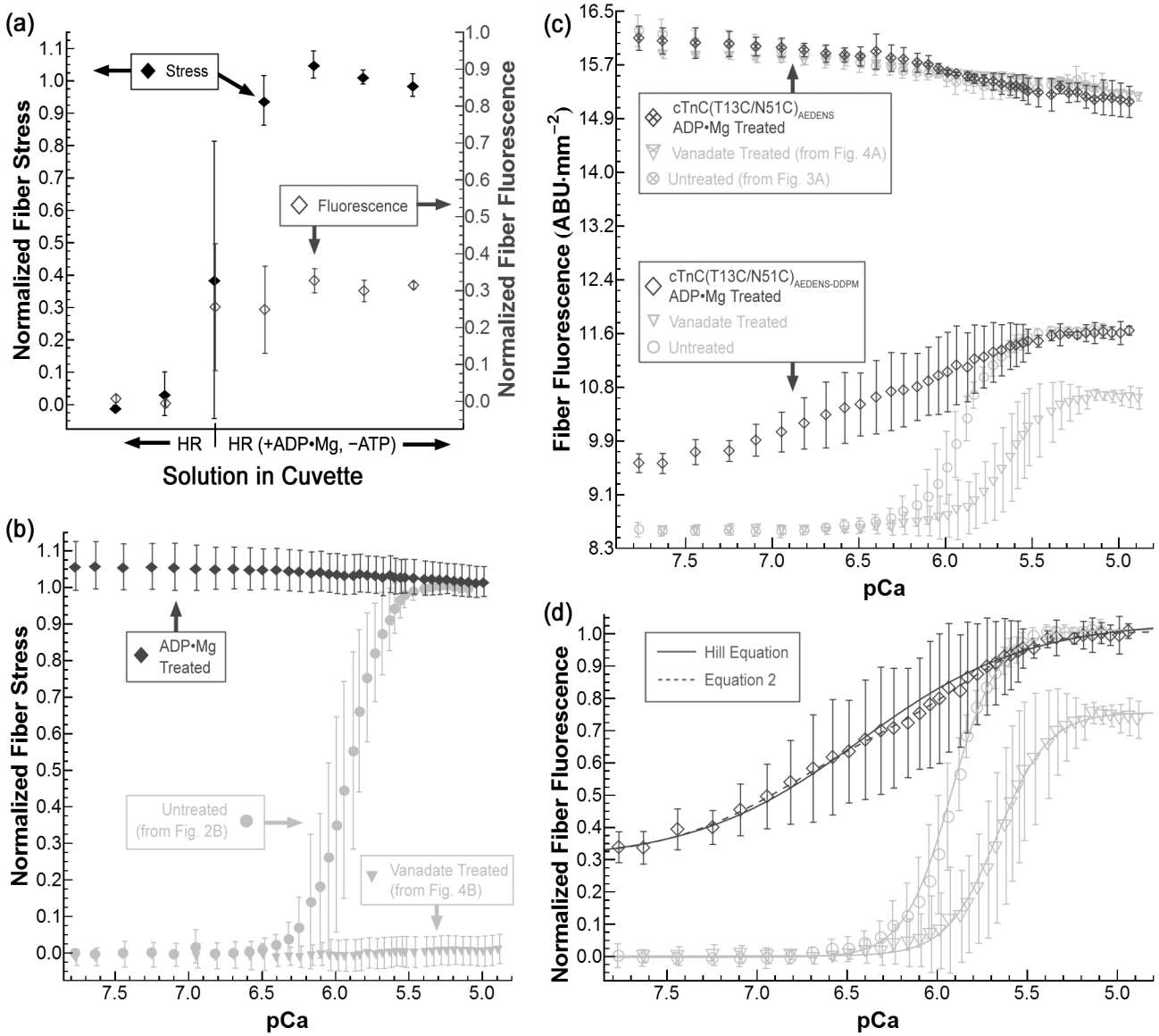

Figure 5.

Use of FRET to determine the effects of ADP•Mg-induced, noncycling strong XBs on N-cTnC opening. (a) Effects of changing the perfusate bathing cTnC(T13C/N51C)$_{AEDENS/DDPM}$ reconstituted fibers (n = 3) from HR to HR+ADP•Mg solutions. Normalization was relative to the initial contraction conducted under normal XB cycling conditions. (b) Fiber stress as a function of pCa observed for cTnC$_{FRET}$-reconstituted fibers (n = 5) treated with 5 mM ADP•Mg in the absence of ATP. (c) Fiber fluorescence as a function of pCa observed for the cTnC$_{FRET}$-reconstituted fibers from panel (b) and ADP-treated, cTnC(T13C/N51C)$_{AEDENS}$-reconstituted fibers (n = 3) (dark gray traces). Fluorescence intensity traces from untreated and Vi-treated fibers are shown for comparison (light gray). (d) Fiber fluorescence intensity data from panel (c) now normalized and fit with the Hill equation. Normalization was done as described in Fig. 4, and Table 2 shows best-fit Hill equation parameters.

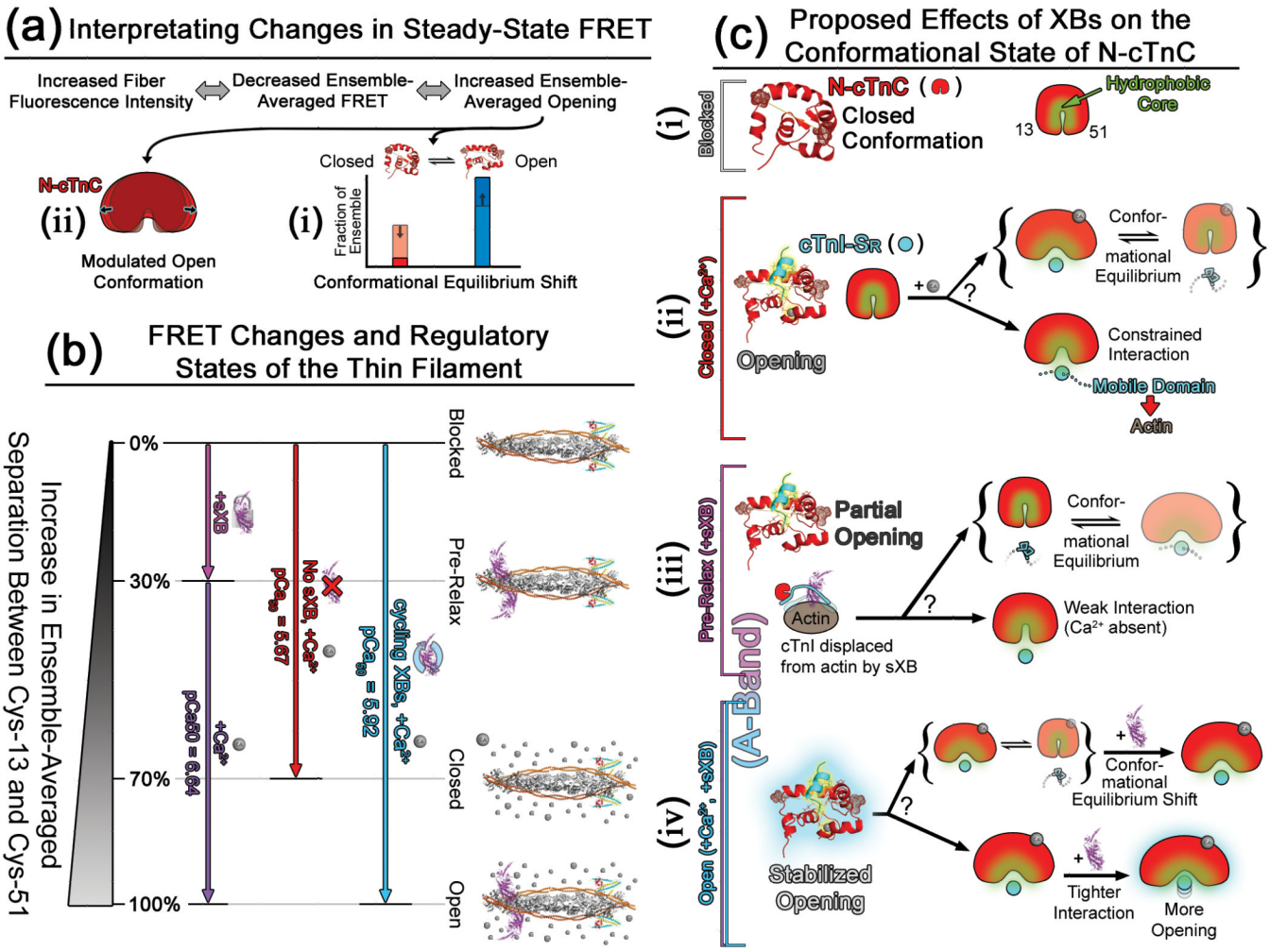

Figure 6.

A summary of the FRET-based insights into the structural effects of strong XBs on the *in situ* conformational behavior of N-cTnC that were found in this study. (a) This schematic emphasizes how the ensemble-averaged FRET data presented in this study is properly interpreted. Increases in ensemble-averaged N-cTnC opening may be reflective of increases in the fraction of the N-cTnC ensemble that is occupying the open conformation (part i). It is also possible that the open conformation itself is being modulated such that a greater extent of the hydrophobic patch is being exposed (part ii). (b) Ensemble-averaged FRET measurements demonstrated that the overall extent of *in situ* N-cTnC opening correlated positively with the Ca^{2+}-sensitivity of CRS and was consistent with the underlying state of TF regulation. Here, increases in the separation between Cys-13 and Cys-51 are relative to the minimal (0% relative hydrophobic patch exposure) and maximal (100% exposure) ensemble-averaged FRET changes observed during the initial contraction and relaxation of untreated, $cTnC_{FRET}$ reconstituted fibers. (c) This diagram depicts the proposed effects of strong XBs on the conformational behavior of N-cTnC as indirectly mediated by cTnI-SR (see related text in *Discussion* section).

Table 1

Isometric stress–Ca^{2+} relationships of myocardial fibers as a function of reconstitution state

Parameter (Hill equation)	Endogenous cTnC (n = 5)	cTnC-depleted (n = 5)	Reconstituted with the following construct:	
			cTnC(wt) (n = 5)	N-cTnC$_{FRET}$ (n = 5)
S_{min} (mN·mm^{-2})[a]	2.96 ± 0.81	2.51 ± 0.52	3.50 ± 1.36	3.43 ± 1.19
S_{max} (mN·mm^{-2})[a]	40.4 ± 2.4	4.39 ± 1.75	36.3 ± 5.5	37.7 ± 5.7
pCa_{50}	5.94 ± 0.03	–	5.93 ± 0.04	5.92 ± 0.03
n_H	3.63 ± 0.28	–	3.29 ± 0.62	3.62 ± 0.45

[a]Determined by averaging the actual passive and maximal stresses of the fibers represented in each respective data set.

Table 2

Ca^{2+}-dependence of *in situ* N-cTnC opening in the absence or presence of XB cycle modulation as monitored in fibers reconstituted with $cTnC_{FRET}$

Parameter (Hill equation)	Chemical modulator of XB cycling		
	None/untreated (n = 5)	1 mM Vi (n = 5)	5 mM Mg·ADP[b] (n = 5)
I_{min}[a]	−0.002 ± 0.006	0.003 ± 0.007	0.298 ± 0.033 *
I_{max}[a]	1.013 ± 0.009	0.687 ± 0.020 *	1.039 ± 0.051
pCa_{50}	5.92 ± 0.02	5.66 ± 0.05 *	6.43 ± 0.11 *
n_H	3.31 ± 0.35	3.06 ± 0.81	0.94 ± 0.21 *

[a] I_{min} and I_{max} refer to minimal and maximal fluorescence intensities. Note that the fluorescence intensities of the data sets appearing in this table have been normalized against the maximal and minimal fluorescence intensities observed for the untreated fiber group.

[b] Note that ATP was not present in the titration solution.

* A statistically significant difference based on a two-tailed Student's *t* test ($p < 0.001$).